NeuroImage: Clinical 22 (2019) 101698

Contents lists available at ScienceDirect

NeuroImage: Clinical

journal homepage: www.elsevier.com/locate/ynicl

Normal Aging Brain Collection Amsterdam (NABCA): A comprehensive collection of postmortem high-field imaging, neuropathological and morphometric datasets of non-neurological controls

Laura E. Jonkman[a,*], Yvon Galis-de Graaf[a], Marjolein Bulk[b,f], Eliane Kaaij[a], Petra J.W. Pouwels[c], Frederik Barkhof[c,d], Annemieke J.M. Rozemuller[e], Louise van der Weerd[b,f], Jeroen J.G. Geurts[a], Wilma D.J. van de Berg[a]

[a] Department of Anatomy and Neurosciences, Amsterdam Neuroscience, Amsterdam UMC, Vrije Universiteit Amsterdam, Amsterdam, the Netherlands
[b] Department of Radiology, Leiden University Medical Centre, Leiden, the Netherlands
[c] Department of radiology and nuclear medicine, Amsterdam Neuroscience, Amsterdam UMC, Vrije Universiteit Amsterdam, Amsterdam, the Netherlands
[d] Institutes of neurology and healthcare engineering, University College London, London, United Kingdom
[e] Department of pathology, Amsterdam Neuroscience, Amsterdam UMC, Vrije Universiteit Amsterdam, Amsterdam, the Netherlands
[f] Department of Human Genetics, Leiden University Medical Centre, Leiden, the Netherlands

ARTICLE INFO

Keywords:
Brain banking
Non-neurological controls
MRI
Neuropathology

ABSTRACT

Well-characterized, high-quality brain tissue of non-neurological control subjects is a prerequisite to study the healthy aging brain, and can serve as a control for the study of neurological disorders. The Normal Aging Brain Collection Amsterdam (NABCA) provides a comprehensive collection of post-mortem (ultra-)high-field MRI (3Tesla and 7 Tesla) and neuropathological datasets of non-neurological controls. By providing MRI within the pipeline, NABCA uniquely stimulates translational neurosciences; from molecular and morphometric tissue studies to the clinical setting. We describe our pipeline, including a description of our on-call autopsy team, donor selection, *in situ* and *ex vivo* post-mortem MRI protocols, brain dissection and neuropathological diagnosis. A demographic, radiological and pathological overview of five selected cases on all these aspects is provided. Additionally, information is given on data management, data and tissue application procedures, including review by a scientific advisory board, and setting up a material transfer agreement before distribution of tissue. Finally, we focus on future prospects, which includes laying the foundation for a unique platform for neuroanatomical, histopathological and neuro-radiological education, of professionals, students and the general (lay) audience.

1. Introduction

1.1. Purpose and mission

A deeper knowledge of the impact of neuropathology on the neuroanatomical circuitry in the aging human brain is required to understand why some people develop highly disabling neurological conditions, whereas others remain neurologically (and mentally) unimpaired until the age of 100 years or more (Ailshire et al., 2015). Well-characterized, high-quality brain tissue of non-neurological control subjects is a prerequisite to study the healthy aging brain, and can serve as a control for the study of neurological disorders. Nevertheless, high-quality post-mortem brain tissue samples of controls without neurological or mental disorders are sparse. To combine willed body donation for medical education and brain donation for research with the same donor, is an efficient opportunity to address both (education and research) needs. Although research groups have included post-mortem MRI in their studies, most notable in the case of patient H.M. (Augustinack et al., 2014), to our knowledge, none of the brain banks worldwide have high-field, whole-brain post-mortem *in situ* magnetic resonance imaging (MRI) data in combination with high quality brain tissue available for scientific research (Daniel and Lees, 1993; Freund et al., 2018; Friedman et al., 2017; Grinberg et al., 2007; Haroutunian and Pickett, 2007; Newcombe and Cuzner, 1993; Rademaker et al., 2018; Ramirez et al., 2018; Ravid and Swaab, 1993; Smith and Millar, 2018; Sutherland et al., 2016; Vonsattel et al., 2008).

* Corresponding author at: VU university medical center, Department of Anatomy and Neurosciences, O|2 building, De Boelelaan 1108, 1081 HZ Amsterdam, The Netherlands.
E-mail address: le.jonkman@vumc.nl (L.E. Jonkman).

https://doi.org/10.1016/j.nicl.2019.101698
Received 3 September 2018; Received in revised form 21 January 2019; Accepted 27 January 2019
Available online 29 January 2019

The Normal Aging Brain Collection Amsterdam (NABCA) answers to this need by providing a comprehensive collection of post-mortem (ultra-)high-field MRI (3Tesla and 7 Tesla) and neuropathological datasets of non-neurological controls. By direct coupling of postmortem MRI and tissue as intrinsic elements of the NABCA collection, we aim to provide the scientific community with a means to translate molecular, cellular, histopathological and brain imaging knowledge to the clinical setting.

NABCA objectives can be summarized as follows:

- Provide the neuroscientific research community (worldwide) with crucially needed, excellently documented, high-quality MRI data and brain tissue of non-neurological controls, for studies of a wide variety of neurological disorders;
- Lay the national foundation for studies of healthy aging, based on a collection of stringently collected brain tissue from 18 to 90 years old;
- Stimulate and innovate translational neurosciences (*i.e.*, translation from molecular and morphometric tissue studies to the clinical setting, *via* advanced post-mortem MR imaging);
- Develop educational neuroanatomical, histopathological and neuroradiological packages for professionals, students and the general (lay) audience.

We have developed a protocol to collect brains of non-neurological donors with a short (4 h–12 h) post-mortem interval (PMI), in combination with uniform and comprehensive characterization with MRI, and histopathology.

1.2. Research site, study population and ethical approval

NABCA is embedded within the department of Anatomy and Neurosciences, Amsterdam Neuroscience, VU University medical center (VUmc). This department has the privilege of administering the human body bequest program. The process of accepting and managing bequests is governed by the human tissue act ('ter beschikking stelling', Artikel 18, lid 1 en 19 van de Wet op de Lijkbezorging, 1991), which allows body donation to facilitate medical research and education. Donors above the age of 18 are eligible to the human body bequest program at VUmc and approximately ~2200 donors are currently registered. In collaboration with the mortuary, NABCA includes ~10 donors a year in the rapid MRI-autopsy pipeline, based on in Section 2.2 mentioned inclusion/exclusion criteria. All medical research on human subjects is ethically and legally guided by the Declaration of Helsinki (https://www.wma.net/policies-post/wma-declaration-of-helsinki-ethical-principles-for-medical-research-involving-human-subjects/). Additionally, NABCA has obtained approval of our institutional ethical review board for all aspects of the pipeline.

2. Autopsy pipeline

Various autopsy pipelines have previously been described (*e.g.*Beach et al., 2015; Bell et al., 2008; Samarasekera et al., 2013). However, NABCA has developed a pipeline that includes *in situ* 3 T and *ex vivo* 7 T MRI as standard practice (see Fig. 1 for an overview). In brief, it starts with donor selection for post-mortem *in situ* 3 T MRI based on age, cause of death and post-mortem delay. The 3 T MRI is evaluated by a neuroradiologist for radiological abnormalities suggestive of neurological disease. After MRI, craniotomy takes place and the brain is photographed and evaluated by a neuropathologist, the weight is noted and fresh snap-frozen tissue excision is performed on the left hemisphere based on an extensive standardized protocol. The right hemisphere is placed in 4% formalin for four weeks, then *ex vivo* scanned at 7 T MRI, and subsequently dissected. In total 35 formalin fixed tissue blocks are collected and embedded in paraffin, the remaining brain tissue is kept in formalin. Histological and immunostained sections of 15 brain regions are evaluated for neuropathological diagnosis, all according to strict standardized protocols in line with BrainNet Europe (BNE) (Alafuzoff et al., 2009b; Alafuzoff et al., 2009a; Alafuzoff et al., 2008). After *in situ* MRI and further brain autopsy, the body is returned to the Anatomy and Neurosciences morgue for further enrolment in the body donation program for education and scientific research. Since 2014, NABCA has so far included over 40 donors. We will explain each of the pipeline aspects in the following paragraphs.

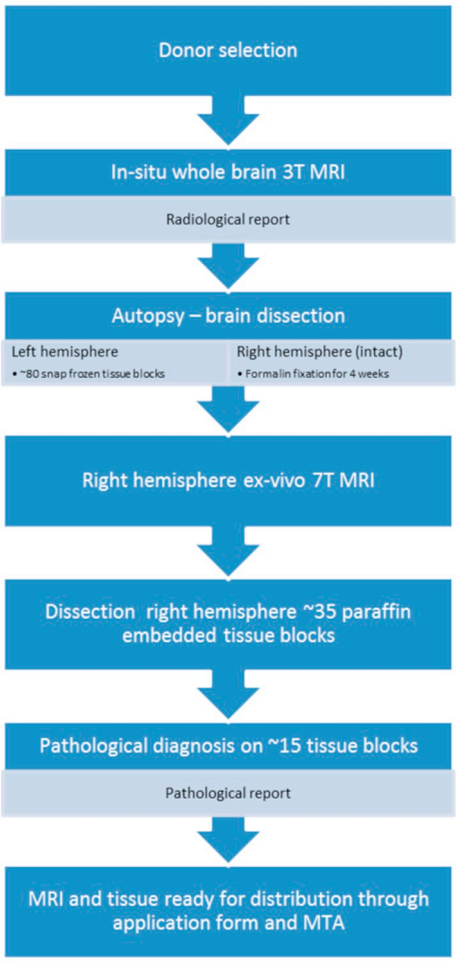

Fig. 1. Overview of NABCA pipeline. Starting with donor selection based on available criteria, an *in situ* MRI is performed. The scan protocol includes a 3D-T1w, PD/T2w and FLAIR sequence (a radiological report of the *in situ* MRI is provided by an experienced radiologist in the days after the scan). After the *in situ* MRI, craniotomy takes place at autopsy, the brain is cut in half; the left hemisphere is dissected in ~80 tissue blocks for molecular and/or biochemical analysis, the right hemisphere is put in 4% formalin. After four weeks, *ex vivo* 7 T MRI is performed on the right hemisphere. The scan protocol includes a 3D-T1w, 3D FLAIR and T2*w sequence. Subsequently the right hemisphere is dissected in 35 tissue blocks for paraffin embedding. Fifteen tissue blocks are then used for a full pathological report provided by an experienced neuropathologist. After this, the non-neurological data is ready for distribution after completion of an application form, approval from the scientific advisory board and institutional review board, and signing of a material transfer agreement (MTA).The NABCA pipeline has been approved by local ethical committee.

2.1. On call MRI and autopsy teams

Previous molecular and biochemical studies using postmortem brain tissue have indicated that post-mortem interval (PMI) has an influence on brain tissue quality (Birdsill et al., 2011; Durrenberger et al., 2010; Ramirez et al., 2018), it therefore is crucial to keep the time between

death and autopsy to a minimum. This can only be achieved by the maintenance of a team that is readily available in case of an autopsy. Before team members become a part of the on-call team, they are trained by means of an extensive introduction and attending an autopsy without assisting. Subsequently, they assist an experienced team member and finally they will join the team as full members. Ongoing meetings are organized to evaluate training needs of team members. For safety and efficiency, at each callout one MRI operator and two autopsy assistants are required. MRI operators and autopsy assistants rotate through a weekly on-call schedule that is planned two months ahead. The neuropathologists have their own on-call schedule at the department of pathology in accordance to other brain banking duties. To expedite the workflow, an autopsy kit is prepared in advance; containers and cassettes are labelled and equipment is laid out ready for use.

2.2. Donor in/exclusion and clinical information

According to the human tissue act, the family of the deceased has up to 24 h to release the body. NABCA only receives a notification (from the VUmc, Anatomy and Neurosciences morgue) if the donor can be at the VUmc morgue within seven hours after death. An exclusion criterion is the cause of death being a neurological or mental disorder, including sepsis, encephalitis, asphyxia, a cerebrovascular accident or traumatic brain injury. Cases with a medical history of neurological or psychiatric diagnosis are excluded too. Furthermore, NABCA focuses on collecting donors above 18 and below 90 years of age. A last exclusion criteria is the presence of neuropathological change at pathological assessment, which will be discussed in Section 2.6.

2.3. Post-mortem in situ 3 T MRI and radiological assessment

When a donor has been included, first an *in situ* MRI (brain still in cranium) is performed on a 3 T whole body scanner (General Electric Signa MR750) using an eight-channel phased-array head coil. The scan protocol (~45 min) is optimized for the post-mortem setting and includes an axial 2D proton density/T2-weighted (PD/T2w) sequence for clinical reference and pathological-anatomical differentiation, a sagittal 3D fluid attenuated inversion recovery (FLAIR) sequence to visualize possible (vascular-ischemic) white and gray matter pathology, a sagittal 3D T1w fast spoiled gradient echo (FSPGR) sequence for gray/white matter differentiation; enabling the study of regional volumes, cortical thickness and shapes, a susceptibility-weighted (T2*w) sequence for iron deposits and microbleeds, and an axial 2D diffusion tensor imaging (DTI; separate reference images with reversed phase encoding directions to estimate and correct susceptibility induced distortions) sequence for microstructural analysis and structural connectivity. See Table 1 for sequence details and Fig. 2 for an example of images. Aside from general post-mortem optimizations, the FLAIR contrast depends on optimal suppression of CSF. However, due to differences in post-mortem delay and brain temperature, T1 relaxation times differ. Therefore, we measure a short series of FLAIR images with low spatial resolution to determine the optimal inversion time per case.

Independent from the autopsy (often the following day), the MRI examination is assessed by an experienced neuroradiologist. The radiological report includes presence of space occupying lesions or other focal/unexpected findings and assessment of atrophy; both global (scale 0–3) and local (scale 0–4), severity of white matter hyperintensities (Fazekas scale 0–3), number of (basal ganglia) lacunar and other infarctions (Fazekas et al., 1987; Wardlaw et al., 2013).

Volumetric analysis of the *in situ* MRI images can be done with processing tools used *in vivo*, such as the FMRIB Software Library (FSL; version 5.0) (Jenkinson et al., 2012). This includes removal of non-brain tissue (BET) on T1-weighted images, and tissue segmentation with SIENAX (Smith et al., 2002) from which normalized volumetric measures are obtained. Additionally, hippocampal volumes are

Table 1
Sequence details of 3 T *in situ* and 7 T *ex vivo* MRI sequences.

Sequence	3 T *in situ*				7 T *ex vivo*			
	PD/T2	3D T1w	FLAIR	DTI	T2*	3D T1	3D FLAIR	T2*
								At different resolutions
Repetition Time (ms)	4250	7	8000	7400	31	4.1	8000	36	36	3140
Echo time (ms)	22/115	3	130	92	25	1.85	298	20	20	25
Inversion time (ms)	–	450	2000–2250	–	–	–	–	–	–	–
Flip Angle (degrees)	–	15	–	–	15	7	–	–	–	–
Acquisition resolution (mm)	0.65 × 0.73 × 3	1x1x1	1.11 × 1.11 × 1.2	2×2×2	0.65 × 0.65 × 3	0.89 × 0.9 × 0.9	0.6 × 0.6 × 0.6	0.6 × 0.6 × 0.6	0.3 × 0.3 × 0.3	0.24 × 0.24 × 1
Reconstructed resolution (mm)	0.5 × 0.5 × 3	0.5 × 0.5 × 1	1x1x1.2	2×2×2	0.5 × 0.5 × 3	0.85 × 0.85 × 0.9	0.3 × 0.3 × 0.6	0.18 × 0.18 × 0.6	0.18 × 0.18 × 0.3	0.21 × 0.21 × 1
Acquisition Time (h:m:s)	4:41	5:07	5:39	4:19	5:00	1:41	1:20:08	21:19	1:54:12	13:18

FLAIR = fluid attenuated inversion recovery; with optimized inversion times per case, due to differences in port-mortem delay and temperature/ Echo-planar imaging (EPI) diffusion tensor imaging (DTI) with b-value 700 s/mm2, 30 gradient directions and 5 b0 reference scans.

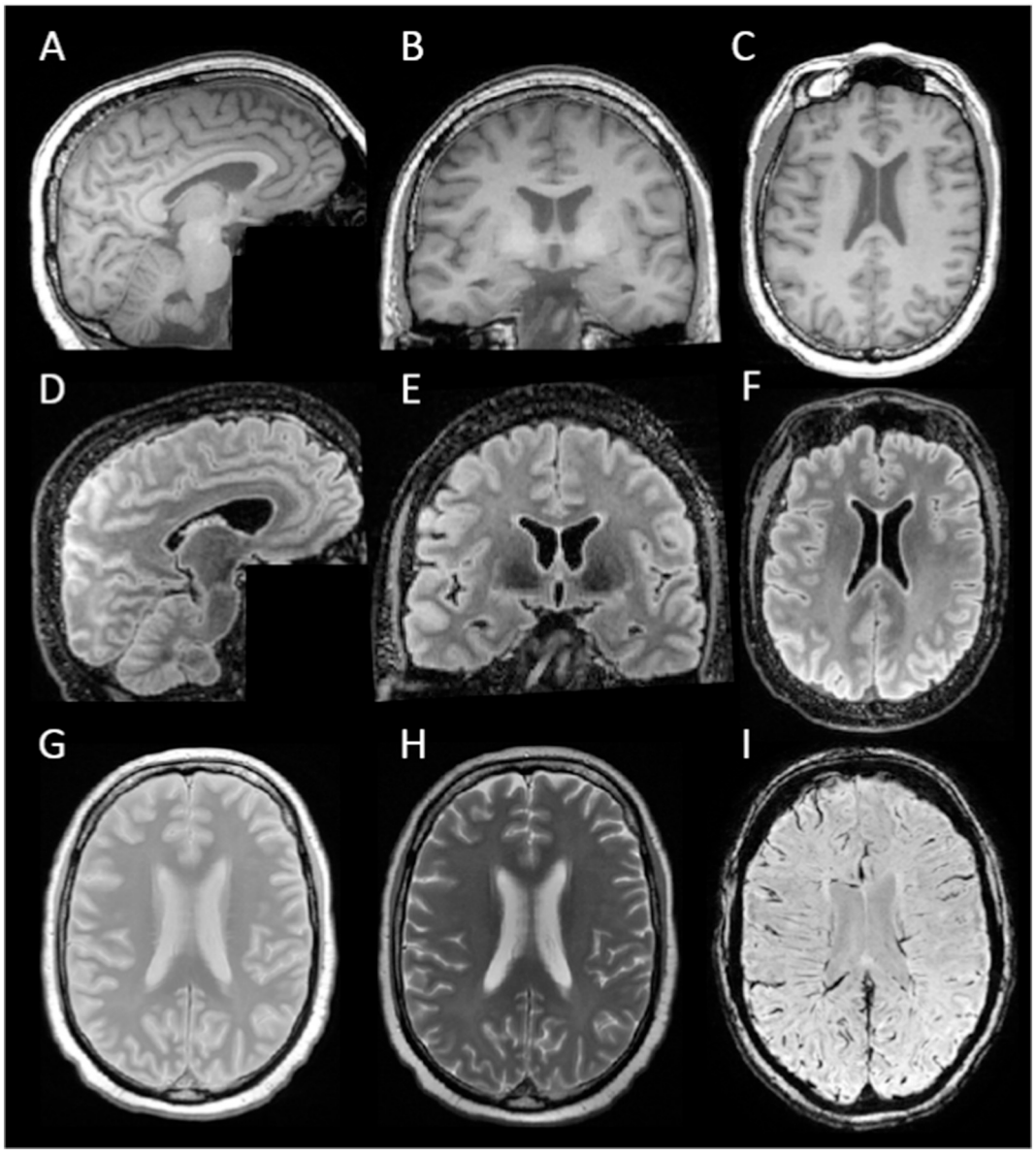

Fig. 2. Overview of images included in the NABCA *in situ* pipeline. Images A-H are from NABCA case 1, age 68, showing no pathological abnormalities, image I is from NABCA case 5, age 59, showing no pathological abnormalities (see Table 3). A-C: sagittal 3D T1w image and reconstructed coronal and axial views, D-F: sagittal 3D FLAIR image and reconstructed coronal and axial views, G: axial 2D proton density (PD) image, H: corresponding axial 2D T2-w image, and I: axial 2D Susceptibility Weighted Image (SWI).

measured with FIRST (also part of FSL (Jenkinson et al., 2012)). See Table 3 for the measurements of 5 non-neurological controls. These volumetric values fall within the range indicative for normal aging in *in vivo* studies (Jack et al., 2015; Scahill et al., 2003).

2.4. Post-mortem ex vivo 7 T MRI

Back in the mortuary, craniotomy takes place and the brain is dissected into two halves; the left hemisphere is further dissected according to a snap frozen protocol (see paragraph 2.5.1), the right hemisphere is stored in 4% formalin.

A higher spatial resolution and signal to noise ratio can be achieved at higher field strengths and longer acquisition times. In addition, 7 T MRI provides unique image contrast compared to the conventional 3 T MRI, particularly for susceptibility-weighted contrast (T_2*w or SWI). These susceptibility-weighted changes are closely related to myelin and iron allowing detection of cortical lamination and iron-associated pathology (Bulk et al., 2018; Nabuurs et al., 2010; van Rooden et al., 2009). Therefore, we include an *ex vivo* 7 T MRI scan, performed at LUMC (Leiden, the Netherlands) on a whole-body human 7 T MR system (Philips Healthcare, Best, the Netherlands) After four weeks of formalin fixation, the right hemisphere is rinsed with tap water for 24 h to partially restore the relaxation parameters (Shepherd et al., 2009). The hemisphere is subsequently sent to LUMC in Phosphate-buffered saline (PBS) and there placed in a plastic bag containing a proton-free fluid (Fomblin®, LC08, Solvay). To minimize the amount of trapped air bubbles, a vacuum is applied overnight. Before scanning, the plastic bag is sealed and fixed on a plastic plateau in the center of the quadrature transmit and 32-channel receiver head coil. The scan protocol (~8 h) includes a coronal 3D T1w scan, and a sagittal 3D FLAIR. Several T_2*w sequences are included with resolutions ranging from lower ($0.6 \times 0.6 \times 0.6$ mm) to higher ($0.3 \times 0.3 \times 0.3$ mm). We acquired *ex vivo* data at different resolutions in order to bridge the gap between *ex vivo* and *in vivo* MRI. *Ex vivo* MRI allows resolutions around 200 um due

to 'unlimited' scan time, in contrast, typical high-resolution scans *in vivo* are acquired at 600 um. Additionally, although fixation drains most of the blood remaining in cerebral vessels, one needs to take into account remaining artefacts when performing quantitative analyses of the T2*w data. See Fig. 3 for an overview of images obtained at 7 T.

2.5. Dissection protocols

After *in situ* MRI, the donor is transported to the morgue and craniotomy takes place. Just before brain removal, the pH of the cerebral spinal fluid (CSF) is measured as an indicator of agonal state (Monoranu et al., 2009). Then the brain, with cervical spinal cord, is delicately removed from the skull by the neuropathologist. Additionally, the pituitary gland is dissected from the sella turcica. The brain is weighted, carefully inspected and photographed from different angles. The autopsy assistants notes the neuropathologist's assessment of the brain's external vasculature (including circle of Willis) and surfaces (*e.g.* atrophy, softening). After this, the cerebellum and brainstem are removed from the cerebrum at the cerebral peduncles. Upon dissection of the brainstem, pigmentation of the substantia nigra (SN) and locus coeruleus (LC) are assessed and noted. The two hemispheres are subsequently split in two; the left hemisphere will be further dissected according to a snap frozen (liquid nitric oxygen) protocol, the right hemisphere will be stored in 4% formalin for four weeks and dissected after 7 T MRI. The same is done for the cerebellum and brain stem. We will briefly discuss both protocols in the following sections. All dissections are performed by an experienced neuropathologists and any salient details at autopsy are written down.

2.5.1. Snap frozen tissue dissection

The snap frozen tissue is stored at -80 °C and may be used for further molecular, biochemical, genetic and cellular analysis. Dissection protocol is based on the BrainNet Europe (BNE) protocol (http://www.brainnet-europe.org/ under "Results", then "Protocols"), and includes ~80 tissue excisions of ~40 brain regions of the cerebrum, cerebellum and brain stem (see supplementary Table 1). Additional to the protocol, two tissue blocks are dissected and snap frozen, one cortical and one cerebellar region. These will later be used to determine the RNA integrity number (RIN), as quality assessment of the frozen tissue (Schroeder et al., 2006).

2.5.2. Formalin fixed tissue dissection

When the formalin fixed right hemisphere is returned from 7 T MRI scanning, the hemisphere is rinsed to dispose of any Fomblin that may still be present. The meninges are carefully removed and the hemisphere is assessed and photographed from all directions with a ruler (any salient details are written down). A coronal cut is made caudal of the anterior commissure, then slices of 0.5 cm thickness are made in both directions (Fig. 4). The formalin fixed dissection protocol includes ~35 regions (see supplementary Table 2). The protocol includes regions for pathological diagnosis (see paragraph 2.6), but is further extended to address specific research needs from researchers requesting tissue from NABCA. The formalin fixed dissected tissue blocks are put in cassettes and are paraffin embedded.

2.6. Neuropathological diagnosis

The last part of the NABCA pipeline involves obtaining a neuropathological diagnosis to ensure they can be considered non-neurological (Nolan et al., 2015). An extensive pathological assessment is done to obtain an overview of age-related or disease-related cellular changes.

From the formalin-fixed dissection, 15 regions (see supplementary Table 3) are selected, and series of 10 × 6-μm-thick sections are cut and mounted onto glass slides. These regions are then stained with

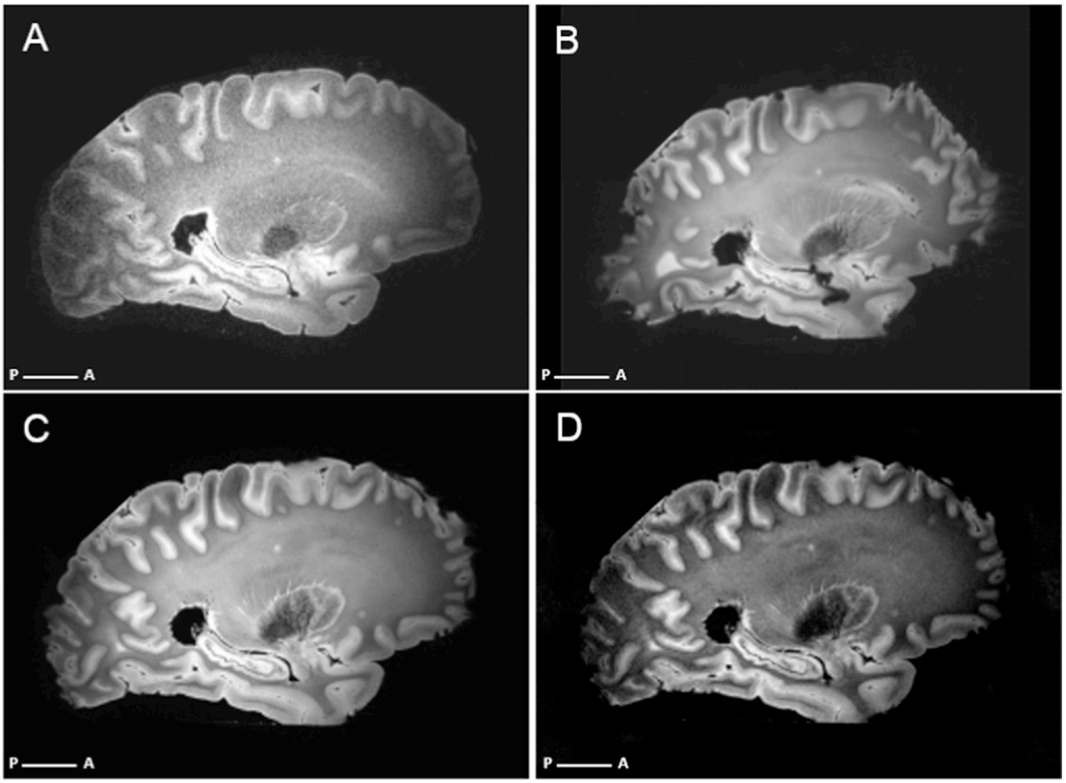

Fig. 3. Overview of sequences included in the NABCA 7 T *ex vivo* pipeline. Images are from NABCA case 1 (see Table 2). A sagittal 3D FLAIR. B-D T2*-weighted scans at different resolutions. B 0.6 × 0.6 × 0.6 mm, C 0.3 × 0.3 × 0.3 mm, D 0.25 × 0.25 × 1mm.

Fig. 4. Overview of a formalin fixed right hemisphere before slice dissection (top) and after dissection into slices. Beginning at the top left, ending at bottom right are 0.5 cm consecutive slices starting at the frontal cortex and moving posteriorly.

(immuno)histochemistry. Manual staining is done for hematoxylin–eosin (HE) for gross anatomical inspection and (micro)infarctions, Congo Red and Gallyas silver staining for plaques, tangles and other inclusions. Automatic staining is done with Ventana Benchmark Ultra (Roche Diagnostics, Mannheim, Germany), with prediluted primary antibodies against hyper phosphorylated (p-)tau for aggregates (including pretangle neurons, neurofibrillary tangles, neuritic plaques, neuropil threads, and dystrophic neurites), α-synuclein to identify Lewy bodies and Lewy-related neurites, Amyloid-β for amyloid deposits, TAR DNA-binding protein 43 (TDP-43) to detect intraneuronal inclusions, and ionized calcium-binding adapter molecule 1 (Iba1) for presence of microglia (see Table 2 for an overview and details).

Pathological assessment is done by an experienced neuropathologist (A.R.) who is blinded to clinical and MRI findings. With the above mentioned staining protocol, an assessment and distinction is made regarding AD-related pathologies, α-synuclein pathologies, TDP-43 pathology, hippocampal sclerosis, vascular pathologies and mixed pathologies (Alafuzoff et al., 2008, 2009a, 2009b; Alafuzoff, 2018; Monoranu et al., 2009; Nag et al., 2015). The extent of AD-related neuropathological burden is summarized by an 'ABC score' according to the 2012 NIA-AA guidelines (Hyman et al., 2012; Montine et al., 2012), which is a composite of 3 scores: (A) stands for Amyloid plaque Thal phase (Thal et al., 2002), (B) stands for Braak stage of NFTs (Braak and Braak, 1991), and (C) stands for Consortium to Establish a Registry for Alzheimer's disease (CERAD) score of neuritic plaques (Hyman et al., 2012). Each criteria is scored on a four-point scale between 0 (no pathology present) and 3 (highest phase/stage/score), and a combination of A, B and C scores represent a 'not', 'low', 'intermediate' or 'high' level of AD-related neuropathological change. An 'intermediate' or 'high' neuropathological change is considered indicative for AD (Hyman et al., 2012; Montine et al., 2012). For staging and typing of Lewy body related α-synuclein pathology, a combination of Braak staging 1 to 6 (Braak et al., 2003) and McKeith typing of brainstem, limbic, neocortical and amygdala-predominant categories (McKeith et al., 2005) is applied, as proposed by BNE (Alafuzoff et al., 2009a). Additionally, brain tissue was also inspected for other salient pathology such as age-related tau astrogliopathy (ARTAG) (Kovacs et al., 2016), cerebral white matter rarefactions, cerebral amyloid angiopathy (CAA) and (micro)infarctions and hemorrhages and TDP pathology (Nag et al., 2015).

NABCA cut-off scores for inclusion as a non-neurological control based on pathology are an 'not' or 'low' classification of AD-related neuropathological change (an 'ABC score' lower than A1 B2 C2), the occurrence of Lewy body pathology higher than Braak stage 3 out of 6 for alphasynucelinopathy (limbic and neocortical), or other salient pathology such as metastases and infarctions or hemorrhages.

2.7. APOE genotyping

For genotyping, 25 mg of tissue is cut from snap-frozen tissue blocks and used for DNA isolation. Frozen material is purified with the PureLink Genomic DNA mini kit (Invitrogen, Carlsbad, California, USA)

Table 2
Technical details of the (immuno)histopathological staining for pathological diagnosis.

Primary	Supplier	Clone	Dilution	Antigen retrieval method
Nissl (Thionine)	Thermo Fisher Scientific	–	–	–
HE	Klinipath/Q-path	–	–	–
Congrored	VWR	–	–	–
Gallyas	Merck KGaA	–	–	–
Anti-Aβ A4	Dako	6f/3d	1:25	CC1: Ventana Benchmark Ultra
Anti-Tau	Innogenetics	AT8	1:10.000	CC1: Ventana Benchmark Ultra
Anti-α-Synuclein	BD Biosciences	42	1:5.000	CC1: Ventana Benchmark Ultra
TDP-43	cosmobio	poly	1:1000	CC1: Ventana Benchmark Ultra
Iba1	Wako Industries	poly	1:4000	CC1: Ventana Benchmark Ultra

Aβ: amyloid-beta; HE: hematoxylin and eosin; Aβ: amyloid-beta; TDP: transactive response DNA-binding protein; Iba1: intracellular calcium binding protein-1; CC1: cell conditioning 1.

Table 3
Demographics, pathological and MRI characteristics of included donors.

ID	Case 1	Case 2	Case 3	Case 4	Case 5	Mean ± SD
Gender	M	F	F	F	F	1 M/4F
Age (y)	68	71	72	77	59	69.4 ± 5.9
PMI (h:m)	8:40	6:50	7:20	4:30	8:10	7:02 ± 1:34
pH of CSF	6.12	6.87	n/a	6.5	6.08	6.39 ± 0.32
Pathological classification “ABC score”	A1 B1 C0	A1 B1 C0	A0 B0 C0	A1 B1 C0	A0 B0 C0	–
Thal phase	2	2	0	2	0	–
Braak NFT	1	0–1	0	2	0	–
Braak a-syn	0	0	0	0	0	–
TDP-43	0	0	0	0	0	–
CAA	0	0	0	0	0	–
APOE-4	E3/E4	E3/E4	E3/E3	E3/E3	E3/E3	–
MTA R/L	0/0	0/1	0/0	1/2	0/0	–
GCA	0	1	0	1	1	–
Fazekas	0	2	1	2	2	–
lacunes	0	0	0	0	0	–
BG lacunes	0	0	0	0	0	–
Infarcts	0	0	0	0	0	–
NBV (L)[a]	1.61	1.48	1.51	1.50	1.46	1.51 ± 0.05
NWMV (L)[a]	0.76	0.71	0.72	0.71	0.68	0.72 ± 0.03
NGMV (L)[a]	0.85	0.77	0.80	0.78	0.78	0.80 ± 0.03
Hippocampus right (ml)[b]	5.31	4.85	6.52	5.20	5.60	5.50 ± 0.57
Hippocampus left (ml)[b]	5.06	5.21	6.35	4.24	5.67	5.31 ± 0.70

M = male, F = female, PMI = post-mortem interval, CSF = cerebrospinal fluid NBV = normalized brain volume, ABC score = score for Aβ deposition (A), for Braak stage of neurofibrillary degeneration (B) and neuritic plaque score (C), NFT = neurofibilary tangles, TDP = TAR DNA-binding protein, CAA = cerebral amyloid angiopathy, APOE = Apolipoprotein E, GCA = global cortical atrophy,BG = basal ganglia, NWMV = normalized white matter volume in litres (L), NGMV = normalized gray matter volume. n/a = not available.

[a] *Normalized volumes obtained with SIENAX.*

[b] *Normalized volumes obtained with FIRST.*

according to manufacturer's protocol. DNA is eluted in 100 μl H_2O and concentration and quality of eluted DNA is measured by nanodrop (ND-1000 spectrometer, Thermo Fisher Scientific Inc., Wilmington, Delaware, USA). Sequencing is performed using Sanger sequencing on an ABI130XL. Subjects are classified as homo- or heterozygote APOEε2, APOEε3 or APOEε4 carriers.

3. Overview of selected cases

To exemplify our pipeline, we have selected five NABCA cases and have put the clinical, MRI, pathological and genotyping data together (see Table 3). On MRI only some mild global or local hippocampal atrophy and mild to moderate vascular white matter changes were observed. Pathologically, the ABC score was not suggestive of Alzheimer pathology for any of the cases. Additionally, case 1 showed some tauopathy in the amygdala, suggestive of ARTAG. Case 4 showed very early stages of α-synucleinopathy (incidental Lewy body pathology), but not enough for a Braak α-syn Stage 1. Case 5 showed a few small cortical infarctions. In summary, these cases showed only minimal age-related changes and can be considered non-neurological controls.

4. Storage and distribution of data and tissue

4.1. Database

NABCA has developed a database and infrastructure for data management. After each autopsy, the database is updated and standardized forms are filled in regarding autopsy details. When more information becomes available about the clinical history, MRI report or pathological diagnosis, this is added to the database. This way, a comprehensive and integrated overview of demographic information (excluding any personal data of the donor), a summary of the medical history, MRI and pathological data is available, as well as an inventory of the snap-frozen and formalin-fixed tissue blocks that were excised. In the near future records of (pending) tissue requests and shipments will be added. Comprehensive search queries can generate various data reports for an overview of available information and tissue. The database is backed up automatically and stored on a secure server. Paper copies of dissection records are saved in a locked filing cabinet.

4.2. Security, privacy and anonymization of data

NABCA works with linked anonymized donors, meaning, family name or other personal data (*e.g.* date of birth or address) of the donor is only available to the head of the morgue (for the human bequest program; information stored in a locked cabinet) and never to people working with NABCA (including CEO, coordinator and on call teams). To NABCA donors are anonymous ID numbers with limited information as shown in Table 3. Regarding MRI scans, brain scans are unique and could allow for identification of the individual (BRAINS (Brain Imaging in Normal Subjects) Expert Working Group et al., 2017), therefore further de-identification of MRI data is applied. Image header information is removed (Rodríguez González et al., 2010), and either defacing (Milchenko and Marcus, 2013), or brain extraction methods (Jenkinson et al., 2012) are applied before distribution.

4.3. Website

NABCA has a website (http://nabca.eu) where contact information and information regarding the application process can be found. In the future, the website will also feature a list with publications that have used NABCA MRI and/or tissue.

4.4. Distribution of data and tissue

Requests for MRI data or tissue can be done through an application form. The application form requires information regarding general information of the applicant, content of the project (summary, background, deliverables, duration), a statement on how the project applies to NABCA objectives, project funding source and possible collaboration with for-profit organizations. Additionally, an overview of the requested data/tissue (number of donors, age range, gender, specific MRI sequences, specific tissue type and locations) is required. This will briefly be reviewed by the NABCA coordinator for completeness and general feasibility/availability. The application will then be sent to NABCA's scientific advisory board which will assess the application based on 1) scientific merit (design, methods, analysis). 2) If the research is in line with the objectives that NABCA is pursuing (see below). 3) originality/innovation. 4) suitability of requested data/tissue (regions, suitable number of donors). The Scientific Advisory Board generally responds with their advice within two weeks after the application has been submitted. Their advice could be to grant the application, grant the application if a few additional points are elucidated, or reject the application in its current form. If the application is rejected, a reason is given. After the Scientific Advisory Board, the application is reviewed by the Institutional Review Board. If their advice is positive, a Material Transfer Agreement (MTA) is signed by both parties, and data/tissue is allocated. Payments are set up to cover replacing of brain tissue with new cases, shipment and handling costs. NABCA has a not-for-profit financial model, there is no monetary gain for staff or institute involved.

5. Discussion, conclusions and future prospects

NABCA's vision is to create a cutting-edge repository of post-mortem non-neurological human brain tissue and post-mortem (ultra-)high-field MR imaging data to national and international researchers, academic and industry. This creates a foundation for the study of healthy aging and as controls for wide variety of neurological disorders, stimulating translational neurosciences, from molecule to mind.

The combination of post-mortem MRI and (immune)histopathology has already proven its great value in the study of prevalent neurodegenerative and neuro-inflammatory diseases (Benveniste et al., 1999; Bulk et al., 2018; Geurts et al., 2005; Gouw et al., 2008; Jonkman et al., 2016; Jonkman and Geurts, 2018; Kilsdonk et al., 2016; Nabuurs et al., 2013; van Veluw et al., 2013). In multiple sclerosis (MS), validation of the pathological substrate of MRI signal changes has led to improvement and implementation of new MRI sequences (Geurts et al., 2011), which in turn helped to improve diagnostic and prognostic accuracy (Filippi et al., 2016). In Alzheimer's disease (AD), histopathological defined cerebral microinfarcts (CMIs) were first detected as hyperintense focal lesions on *ex vivo* 7 T MRI, then on *in vivo* 7 T MRI in the same study (van Veluw et al., 2013) and subsequently on *in vivo* 3 T MRI, which could be related to clinical phenotype (cognitive impairment) (Ferro et al., 2017; Hilal et al., 2016). Additionally, the combination of post-mortem MRI and histology has played a crucial role in creating and validating several (cortical and subcortical) anatomical atlases (Adler et al., 2018; Chakravarty et al., 2006; Ewert et al., 2018; Yelnik et al., 2007; Yushkevich et al., 2009), or software packages (Cardinale et al., 2014). In the future, *in situ* MRI could play an essential role as an intermediate between *ex vivo* and *in vivo* registration and validation (Wisse et al., 2016). Additionally, studies regarding validation of new MRI sequences and development of MRI biomarkers will increase and continue to require post-mortem tissue validation. Lastly, the combination of molecular/biochemical, histopathological and 3D neuroanatomical (at macroscale and microscale) of the same donor allows answering questions regarding impact of molecular changes or pathological lesions on anatomical circuitry.

Nevertheless, some limitations can be mentioned about the pipeline. Donors enrolled for NABCA, or the body bequest program in general, may not be an accurate representation of the entire (Dutch) population. Due to personal or religious feelings, the population may lack some diversity. In addition, few young adult donors have been included to date. Information regarding the medical history may be limited or sometimes lacking (general practitioners have the right not to disclose patients' information). The MRI sequences may be limited and not at par to a researcher's need, but NABCA continues to develop and include more advanced imaging techniques. Additionally, tissue quality is an important aspect and the RNA integrity number (RIN) of all specimens is collected. For biochemical and next-generation sequencing however other quality measures may need to be included.

In the future NABCA would like to (i) add morphometric data to imaging and histology, such as size, shape and distribution of neurons, axons and pathological hallmarks. (ii) Add more genotyping data such as amyloid precursor protein (APP), presenilin-1 (PS-1) and presenilin-2 (PS-2), leucine rich repeat kinase 2 (LRRK2), glucocerebrosidase (GBA), synuclein alpha (SNCA) multiplication and others (Blauwendraat et al., 2017). (iii) feed data (*e.g.* molecular information) from research teams using NABCA data back into the database (iv) lay the foundation for a unique platform for neuroanatomical, histopathological and neuroradiological education, of professionals, students and the general (lay) audience. For instance by organizing (summer)courses and lectures based on NABCA's multimodal datasets. Additionally, in the development of new ways of visualizing brain structure, NABCA is collaborating with researchers who are developing an app together with the gaming industry, VU University Medical Center's 3D Innovation Lab and a scientific team from Delft Technical University. This app will feature the multimodal (MRI, anatomy and molecular data) normal brain repository. Besides professionals and the scientific community, the general audience is extremely interested in brain science as well explaining the recent success of 'brain books' for the layperson and *e.g.* outreach organizations such as 'Brein in Beeld' (http://breininbeeld.org; outreach ~2500 people). The education of the scientific community and general public alike will not only improve the general knowledge on the aging human brain, but will also increase awareness of the importance of studying human tissue and brain banking in general.

In conclusion, the immense scope of modalities and techniques involved (*i.e.* molecular, cellular, network imaging) is unprecedented and NABCA forms a unique platform for translational neuroscience research and education.

Funding

This work was supported by Amsterdam Neuroscience, Netherlands [1-BI-2013 and 1-PoC-BI-2017]. FB is supported by the NIHR biomedical research centre at UCLH.

Acknowledgements

The authors wish to express their immense gratitude to all the donors of the body donation program. Additionally we would like to thank the NABCA MRI and autopsy teams for their continuing efforts. Specifically we would like to thank Alexandra Weeber and Roel Klaver for their efforts in developing standard operating protocols for post-mortem tissue analysis, Martijn Steenwijk for 3 T *in situ* scanning, Mathijs Buijs for *ex vivo* 7 T scanning, Marianne Bugiani for additional pathological dissections, Evelien Timmermans and John Bol for designing the database. Funding: This work was supported by Amsterdam Neuroscience, Netherlands [grant year 2013 and 1-PoC-BI-2017]. FB is supported by the NIHR biomedical research centre at UCLH.

Appendix A. Supplementary data

Supplementary data to this article can be found online at https://doi.org/10.1016/j.nicl.2019.101698.

References

Adler, D.H., Wisse, L.E.M., Ittyerah, R., Pluta, J.B., Ding, S.-L., Xie, L., Wang, J., Kadivar, S., Robinson, J.L., Schuck, T., Trojanowski, J.Q., Grossman, M., Detre, J.A., Elliott, M.A., Toledo, J.B., Liu, W., Pickup, S., Miller, M.I., Das, S.R., Wolk, D.A., Yushkevich, P.A., 2018. Characterizing the human hippocampus in aging and Alzheimer's disease using a computational atlas derived from ex vivo MRI and histology. Proc. Natl. Acad. Sci. 115, 4252–4257. https://doi.org/10.1073/pnas.1801093115.

Ailshire, J.A., Beltran-Sanchez, H., Crimmins, E.M., 2015. Becoming Centenarians: disease and functioning trajectories of older U.S. adults as they survive to 100. J. Gerontol. Ser. A Biol. Sci. Med. Sci. 70, 193–201. https://doi.org/10.1093/gerona/glu124.

Alafuzoff, I., 2018. Minimal neuropathologic diagnosis for brain banking in the normal middle-aged and aged brain and in neurodegenerative disorders. Handb. Clin. Neurol. 131–141. https://doi.org/10.1016/B978-0-444-63639-3.00010-4.

Alafuzoff, I., Arzberger, T., Al-Sarraj, S., Bodi, I., Bogdanovic, N., Braak, H., Bugiani, O., Del-Tredici, K., Ferrer, I., Gelpi, E., Giaccone, G., Graeber, M.B., Ince, P., Kamphorst, W., King, A., Korkolopoulou, P., Kovács, G.G., Larionov, S., Meyronet, D., Monoranu, C., Parchi, P., Patsouris, E., Roggendorf, W., Seilhean, D., Tagliavini, F., Stadelmann, C., Streichenberger, N., Thal, D.R., Wharton, S.B., Kretzschmar, H., 2008. Staging of neurofibrillary pathology in Alzheimer's disease: a study of the BrainNet Europe consortium. Brain Pathol. https://doi.org/10.1111/j.1750-3639.2008.00147.x. 0, 080509082911413–???.

Alafuzoff, I., Ince, P.G., Arzberger, T., Al-Sarraj, S., Bell, J., Bodi, I., Bogdanovic, N., Bugiani, O., Ferrer, I., Gelpi, E., Gentleman, S., Giaccone, G., Ironside, J.W., Kavantzas, N., King, A., Korkolopoulou, P., Kovács, G.G., Meyronet, D., Monoranu, C., Parchi, P., Parkkinen, L., Patsouris, E., Roggendorf, W., Rozemuller, A., Stadelmann-Nessler, C., Streichenberger, N., Thal, D.R., Kretzschmar, H., 2009a. Staging/typing of Lewy body related α-synuclein pathology: a study of the BrainNet Europe Consortium. Acta Neuropathol. 117, 635–652. https://doi.org/10.1007/s00401-009-0523-2.

Alafuzoff, I., Thal, D.R., Arzberger, T., Bogdanovic, N., Al-Sarraj, S., Bodi, I., Boluda, S., Bugiani, O., Duyckaerts, C., Gelpi, E., Gentleman, S., Giaccone, G., Graeber, M., Hortobagyi, T., Höftberger, R., Ince, P., Ironside, J.W., Kavantzas, N., King, A., Korkolopoulou, P., Kovács, G.G., Meyronet, D., Monoranu, C., Nilsson, T., Parchi, P., Patsouris, E., Pikkarainen, M., Revesz, T., Rozemuller, A., Seilhean, D., Schulz-Schaeffer, W., Streichenberger, N., Wharton, S.B., Kretzschmar, H., 2009b. Assessment of β-amyloid deposits in human brain: a study of the BrainNet Europe Consortium. Acta Neuropathol. 117, 309–320. https://doi.org/10.1007/s00401-009-0485-4.

Augustinack, J.C., van der Kouwe, A.J.W., Salat, D.H., Benner, T., Stevens, A.A., Annese, J., Fischl, B., Frosch, M.P., Corkin, S., 2014. H.M.'s contributions to neuroscience: a review and autopsy studies. Hippocampus 24, 1267–1286. https://doi.org/10.1002/hipo.22354.

Beach, T.G., Adler, C.H., Sue, L.I., Serrano, G., Shill, H.A., Walker, D.G., Lue, L., Roher, A.E., Dugger, B.N., Maarouf, C., Birdsill, A.C., Intorcia, A., Saxon-Labelle, M., Pullen, J., Scroggins, A., Filon, J., Scott, S., Hoffman, B., Garcia, A., Caviness, J.N., Hentz, J.G., Driver-Dunckley, E., Jacobson, S.A., Davis, K.J., Belden, C.M., Long, K.E., Malek-Ahmadi, M., Powell, J.J., Gale, L.D., Nicholson, L.R., Caselli, R.J., Woodruff, B.K., Rapscak, S.Z., Ahern, G.L., Shi, J., Burke, A.D., Reiman, E.M., Sabbagh, M.N., 2015. Arizona study of aging and neurodegenerative disorders and brain and body donation program. Neuropathology 35, 354–389. https://doi.org/10.1111/neup.12189.

Bell, J.E., Alafuzoff, I., Al-Sarraj, S., Arzberger, T., Bogdanovic, N., Budka, H., Dexter, D.T., Falkai, P., Ferrer, I., Gelpi, E., Gentleman, S.M., Giaccone, G., Huitinga, I., Ironside, J.W., Kliouevа, N., Kovacs, G.G., Meyronet, D., Palkovits, M., Parchi, P., Patsouris, E., Reynolds, R., Riederer, P., Roggendorf, W., Seilhean, D., Schmitt, A., Schmitz, P., Streichenberger, N., Schwalber, A., Kretzschmar, H., 2008. Management of a twenty-first century brain bank: experience in the BrainNet Europe consortium. Acta Neuropathol. 115, 497–507. https://doi.org/10.1007/s00401-008-0360-8.

Benveniste, H., Einstein, G., Kim, K.R., Hulette, C., Johnson, G.A., 1999. Detection of neuritic plaques in Alzheimer's disease by magnetic resonance microscopy. Proc. Natl. Acad. Sci. U. S. A. 96, 14079–14084.

Birdsill, A.C., Walker, D.G., Lue, L., Sue, L.I., Beach, T.G., 2011. Postmortem interval effect on RNA and gene expression in human brain tissue. Cell Tissue Bank. 12, 311–318. https://doi.org/10.1007/s10561-010-9210-8.

Blauwendraat, C., Faghri, F., Pihlstrom, L., Geiger, J.T., Elbaz, A., Lesage, S., Corvol, J.-C., May, P., Nicolas, A., Abramzon, Y., Murphy, N.A., Gibbs, J.R., Ryten, M., Ferrari, R., Bras, J., Guerreiro, R., Williams, J., Sims, R., Lubbe, S., Hernandez, D.G., Mok, K.Y., Robak, L., Campbell, R.H., Rogaeva, E., Traynor, B.J., Chia, R., Chung, S.J., International Parkinson's disease genomics consortium (IPDGC), COURAGE-PD consortium, Hardy, J.A., Brice, A., Wood, N.W., Houlden, H., Shulman, J.M., Morris, H.R., Gasser, T., Krüger, R., Heutink, P., Sharma, M., Simón-Sánchez, J., Nalls, M.A., Singleton, A.B., Scholz, S.W., 2017. NeuroChip, an updated version of the NeuroX genotyping platform to rapidly screen for variants associated with neurological diseases. Neurobiol. Aging 57https://doi.org/10.1016/j.neurobiolaging.2017.05.009.247.e9–247.e13.

Braak, H., Braak, E., 1991. Neuropathological stageing of Alzheimer-related changes. Acta Neuropathol. 82, 239–259.

Braak, H., Del Tredici, K., Rüb, U., de Vos, R.A., Jansen Steur, E.N., Braak, E., 2003. Staging of brain pathology related to sporadic Parkinson's disease. Neurobiol. Aging 24, 197–211. https://doi.org/10.1016/S0197-4580(02)00065-9.

BRAINS (Brain Imaging in Normal Subjects) Expert Working Group, B. (Brain I. in N.S.E.W.), Shenkin, S.D., Pernet, C., Nichols, T.E., Poline, J.-B., Matthews, P.M., van der Lugt, A., Mackay, C., Lanyon, L., Mazoyer, B., Boardman, J.P., Thompson, P.M., Fox, N., Marcus, D.S., Sheikh, A., Cox, S.R., Anblagan, D., Job, D.E., Dickie, D.A., Rodriguez, D., Wardlaw, J.M., 2017. Improving data availability for brain image biobanking in healthy subjects: Practice-based suggestions from an international multidisciplinary working group. NeuroImage 153, 399–409. https://doi.org/10.1016/j.neuroimage.2017.02.030.

Bulk, M., Abdelmoula, W.M., Nabuurs, R.J.A., van der Graaf, L.M., Mulders, C.W.H., Mulder, A.A., Jost, C.R., Koster, A.J., van Buchem, M.A., Natté, R., Dijkstra, J., van der Weerd, L., 2018. Postmortem MRI and histology demonstrate differential iron accumulation and cortical myelin organization in early- and late-onset Alzheimer's disease. Neurobiol. Aging 62, 231–242. https://doi.org/10.1016/j.neurobiolaging.2017.10.017.

Cardinale, F., Chinnici, G., Bramerio, M., Mai, R., Sartori, I., Cossu, M., Lo Russo, G., Castana, L., Colombo, N., Caborni, C., De Momi, E., Ferrigno, G., 2014. Validation of freesurfer-estimated brain cortical thickness: comparison with histologic measurements. Neuroinformatics 12, 535–542. https://doi.org/10.1007/s12021-014-9229-2.

Chakravarty, M.M., Bertrand, G., Hodge, C.P., Sadikot, A.F., Collins, D.L., 2006. The creation of a brain atlas for image guided neurosurgery using serial histological data. NeuroImage 30, 359–376. https://doi.org/10.1016/J.NEUROIMAGE.2005.09.041.

Daniel, S.E., Lees, A.J., 1993. Parkinson's disease society Brain Bank, London: overview and research. J. Neural Transm. Suppl. 39, 165–172.

Durrenberger, P.F., Fernando, S., Kashefi, S.N., Ferrer, I., Hauw, J.-J., Seilhean, D., Smith, C., Walker, R., Al-Sarraj, S., Troakes, C., Palkovits, M., Kasztner, M., Huitinga, I., Arzberger, T., Dexter, D.T., Kretzschmar, H., Reynolds, R., 2010. Effects of antemortem and postmortem variables on human brain mRNA QUALITY: a BrainNet Europe Study. J. Neuropathol. Exp. Neurol. 69, 70–81. https://doi.org/10.1097/NEN.0b013e3181c7e32f.

Ewert, S., Plettig, P., Li, N., Chakravarty, M.M., Collins, D.L., Herrington, T.M., Kühn, A.A., Horn, A., 2018. Toward defining deep brain stimulation targets in MNI space: a subcortical atlas based on multimodal MRI, histology and structural connectivity. NeuroImage 170, 271–282. https://doi.org/10.1016/j.neuroimage.2017.05.015.

Fazekas, F., Chawluk, J., Alavi, A., Hurtig, H., Zimmerman, R., 1987. MR signal abnormalities at 1.5 T in Alzheimer's dementia and normal aging. Am. J. Roentgenol. 149, 351–356. https://doi.org/10.2214/ajr.149.2.351.

Ferro, D.A., van Veluw, S.J., Koek, H.L., Exalto, L.G., Biessels, G.J., Utrecht Vascular Cognitive Impairment (VCI) study group, 2017. Cortical Cerebral Microinfarcts on 3 Tesla MRI in patients with Vascular Cognitive Impairment. J. Alzheimers Dis. 60, 1443–1450. https://doi.org/10.3233/JAD-170481.

Filippi, M., Rocca, M.A., Ciccarelli, O., De Stefano, N., Evangelou, N., Kappos, L., Rovira, A., Sastre-Garriga, J., Tintorè, M., Frederiksen, J.L., Gasperini, C., Palace, J., Reich, D.S., Banwell, B., Montalban, X., Barkhof, F., MAGNIMS Study Group, 2016. MRI criteria for the diagnosis of multiple sclerosis: MAGNIMS consensus guidelines. Lancet Neurol. 15, 292–303. https://doi.org/10.1016/S1474-4422(15)00393-2.

Freund, M., Taylor, A., Ng, C., Little, A.R., 2018. The NIH NeuroBioBank: creating opportunities for human brain research. Handb. Clin. Neurol. 41–48. https://doi.org/10.1016/B978-0-444-63639-3.00004-9.

Friedman, M.J., Huber, B.R., Brady, C.B., Ursano, R.J., Benedek, D.M., Kowall, N.W., McKee, A.C., Traumatic Stress Brain Research Group, 2017. VA's National PTSD Brain Bank: a National Resource for Research. Curr. Psychiatr. Rep. 19, 73. https://doi.org/10.1007/s11920-017-0822-6.

Geurts, J.J.G., Bö, L., Pouwels, P.J.W., Castelijns, J.A., Polman, C.H., Barkhof, F., 2005. Cortical lesions in multiple sclerosis: combined postmortem MR imaging and histopathology. AJNR Am. J. Neuroradiol. 26, 572–577.

Geurts, J.J.G., Roosendaal, S.D., Calabrese, M., Ciccarelli, O., Agosta, F., Chard, D.T.,

Gass, A., Huerga, E., Moraal, B., Pareto, D., Rocca, M.A., Wattjes, M.P., Yousry, T.A., Uitdehaag, B.M.J., Barkhof, F., 2011. Consensus recommendations for MS cortical lesion scoring using double inversion recovery MRI. Neurology 76, 418–424. https://doi.org/10.1212/WNL.0b013e31820a0cc4.

Gouw, A.A., Seewann, A., Vrenken, H., van der Flier, W.M., Rozemuller, J.M., Barkhof, F., Scheltens, P., Geurts, J.J.G., 2008. Heterogeneity of white matter hyperintensities in Alzheimer's disease: post-mortem quantitative MRI and neuropathology. Brain 131, 3286–3298. https://doi.org/10.1093/brain/awn265.

Grinberg, L.T., de Lucena Ferretti, R.E., Farfel, J.M., Leite, R., Pasqualucci, C.A., Rosemberg, S., Nitrini, R., Saldiva, P.H.N., Jacob Filho, W., Brazilian Aging Brain Study Group, 2007. Brain Bank of the Brazilian aging brain study group—a milestone reached and more than 1,600 collected brains. Cell Tissue Bank. 8, 151–162. https://doi.org/10.1007/s10561-006-9022-z.

Haroutunian, V., Pickett, J., 2007. Autism brain tissue banking. Brain Pathol. 17, 412–421. https://doi.org/10.1111/j.1750-3639.2007.00097.x.

Hilal, S., Sikking, E., Shaik, M.A., Chan, Q.L., van Veluw, S.J., Vrooman, H., Cheng, C.-Y., Sabanayagam, C., Cheung, C.Y., Wong, T.Y., Venketasubramanian, N., Biessels, G.J., Chen, C., Ikram, M.K., 2016. Cortical cerebral microinfarcts on 3T MRI. Neurology 87, 1583–1590. https://doi.org/10.1212/WNL.0000000000003110.

Hyman, B.T., Phelps, C.H., Beach, T.G., Bigio, E.H., Cairns, N.J., Carrillo, M.C., Dickson, D.W., Duyckaerts, C., Frosch, M.P., Masliah, E., Mirra, S.S., Nelson, P.T., Schneider, J.A., Thal, D.R., Thies, B., Trojanowski, J.Q., Vinters, H.V., Montine, T.J., 2012. National Institute on Aging-Alzheimer's Association guidelines for the neuropathologic assessment of Alzheimer's disease. Alzheimers Dement. 8, 1–13. https://doi.org/10.1016/j.jalz.2011.10.007.

Jack, C.R., Wiste, H.J., Weigand, S.D., Knopman, D.S., Mielke, M.M., Vemuri, P., Lowe, V., Senjem, M.L., Gunter, J.L., Reyes, D., Machulda, M.M., Roberts, R., Petersen, R.C., 2015. Different definitions of neurodegeneration produce similar amyloid/neurodegeneration biomarker group findings. Brain 138, 3747–3759. https://doi.org/10.1093/brain/awv283.

Jenkinson, M., Beckmann, C.F., Behrens, T.E.J., Woolrich, M.W., Smith, S.M., 2012. FSL. NeuroImage 62, 782–790. https://doi.org/10.1016/j.neuroimage.2011.09.015.

Jonkman, L.E., Geurts, J.J.G., 2018. Postmortem magnetic resonance imaging. Handb. Clin. Neurol. 335–354. https://doi.org/10.1016/B978-0-444-63639-3.00023-2.

Jonkman, L.E., Klaver, R., Fleysher, L., Inglese, M., Geurts, J.J., 2016. The substrate of increased cortical FA in MS: a 7T post-mortem MRI and histopathology study. Mult. Scler. https://doi.org/10.1177/1352458516635290.

Kilsdonk, I.D., Jonkman, L.E., Klaver, R., van Veluw, S.J., Zwanenburg, J.J.M., Kuijer, J.P.A., Pouwels, P.J.W., Twisk, J.W.R., Wattjes, M.P., Luijten, P.R., Barkhof, F., Geurts, J.J.G., 2016. Increased cortical grey matter lesion detection in multiple sclerosis with 7 T MRI: a post-mortem verification study. Brain. https://doi.org/10.1093/brain/aww037.

Kovacs, G.G., Ferrer, I., Grinberg, L.T., Alafuzoff, I., Attems, J., Budka, H., Cairns, N.J., Crary, J.F., Duyckaerts, C., Ghetti, B., Halliday, G.M., Ironside, J.W., Love, S., Mackenzie, I.R., Munoz, D.G., Murray, M.E., Nelson, P.T., Takahashi, H., Trojanowski, J.Q., Ansorge, O., Arzberger, T., Baborie, A., Beach, T.G., Bieniek, K.F., Bigio, E.H., Bodi, I., Dugger, B.N., Feany, M., Gelpi, E., Gentleman, S.M., Giaccone, G., Hatanpaa, K.J., Heale, R., Hof, P.R., Hofer, M., Hortobágyi, T., Jellinger, K., Jicha, G.A., Ince, P., Kofler, J., Kövari, E., Kril, J.J., Mann, D.M., Matej, R., McKee, A.C., McLean, C., Milenkovic, I., Montine, T.J., Murayama, S., Lee, E.B., Rahimi, J., Rodriguez, R.D., Rozemüller, A., Schneider, J.A., Schultz, C., Seeley, W., Seilhean, D., Smith, C., Tagliavini, F., Takao, M., Thal, D.R., Toledo, J.B., Tolnay, M., Troncoso, J.C., Vinters, H.V., Weis, S., Wharton, S.B., White, C.L., Wisniewski, T., Woulfe, J.M., Yamada, M., Dickson, D.W., 2016. Aging-related tau astrogliopathy (ARTAG): harmonized evaluation strategy. Acta Neuropathol. 131, 87–102. https://doi.org/10.1007/s00401-015-1509-x.

McKeith, I.G., Dickson, D.W., Lowe, J., Emre, M., O'Brien, J.T., Feldman, H., Cummings, J., Duda, J.E., Lippa, C., Perry, E.K., Aarsland, D., Arai, H., Ballard, C.G., Boeve, B., Burn, D.J., Costa, D., Del Ser, T., Dubois, B., Galasko, D., Gauthier, S., Goetz, C.G., Gomez-Tortosa, E., Halliday, G., Hansen, L.A., Hardy, J., Iwatsubo, T., Kalaria, R.N., Kaufer, D., Kenny, R.A., Korczyn, A., Kosaka, K., Lee, V.M.Y., Lees, A., Litvan, I., Londos, E., Lopez, O.L., Minoshima, S., Mizuno, Y., Molina, J.A., Mukaetova-Ladinska, E.B., Pasquier, F., Perry, R.H., Schulz, J.B., Trojanowski, J.Q., Yamada, M., Consortium on DLB, 2005. Diagnosis and management of dementia with Lewy bodies: Third report of the DLB consortium. Neurology 65, 1863–1872. https://doi.org/10.1212/01.wnl.0000187889.17253.b1.

Milchenko, M., Marcus, D., 2013. Obscuring surface anatomy in volumetric imaging data. Neuroinformatics 11, 65–75. https://doi.org/10.1007/s12021-012-9160-3.

Monoranu, C.M., Apfelbacher, M., Grünblatt, E., Puppe, B., Alafuzoff, I., Ferrer, I., Al-Saraj, S., Keyvani, K., Schmitt, A., Falkai, P., Schittenhelm, J., Halliday, G., Kril, J., Harper, C., McLean, C., Riederer, P., Roggendorf, W., 2009. pH measurement as quality control on human post mortem brain tissue: a study of the BrainNet Europe consortium. Neuropathol. Appl. Neurobiol. 35, 329–337. https://doi.org/10.1111/j.1365-2990.2008.01003a.x.

Montine, T.J., Phelps, C.H., Beach, T.G., Bigio, E.H., Cairns, N.J., Dickson, D.W., Duyckaerts, C., Frosch, M.P., Masliah, E., Mirra, S.S., Nelson, P.T., Schneider, J.A., Thal, D.R., Trojanowski, J.Q., Vinters, H.V., Hyman, B.T., National Institute on Aging, Alzheimer's Association, 2012. National institute on aging-Alzheimer's association guidelines for the neuropathologic assessment of Alzheimer's disease: a practical approach. Acta Neuropathol. 123, 1–11. https://doi.org/10.1007/s00401-011-0910-3.

Nabuurs, R.J.A., Hegeman, I., Natté, R., van Duinen, S.G., van Buchem, M.A., van der Weerd, L., Webb, A.G., 2010. High-field MRI of single histological slices using an inductively coupled, self-resonant microcoil: application to ex vivo samples of patients with Alzheimer's disease. NMR Biomed. 24https://doi.org/10.1002/nbm.1598. n/a-n/a.

Nabuurs, R.J.A., Natté, R., de Ronde, F.M., Hegeman-Kleinn, I., Dijkstra, J., van Duinen, S.G., Webb, A.G., Rozemuller, A.J., van Buchem, M.A., van der Weerd, L., 2013. MR microscopy of human amyloid-β deposits: characterization of parenchymal amyloid, diffuse plaques, and vascular amyloid. J. Alzheimers Dis. 34, 1037–1049. https://doi.org/10.3233/JAD-122215.

Nag, S., Yu, L., Capuano, A.W., Wilson, R.S., Leurgans, S.E., Bennett, D.A., Schneider, J.A., 2015. Hippocampal sclerosis and TDP-43 pathology in aging and Alzheimer disease. Ann. Neurol. 77, 942–952. https://doi.org/10.1002/ana.24388.

Newcombe, J., Cuzner, M.L., 1993. Organization and research applications of the U.K. Multiple Sclerosis Society Tissue Bank. J. Neural Transm. Suppl. 39, 155–163.

Nolan, M., Troakes, C., King, A., Bodi, I., Al-Sarraj, S., 2015. Control tissue in brain banking: the importance of thorough neuropathological assessment. J. Neural Transm. 122, 949–956. https://doi.org/10.1007/s00702-015-1376-6.

Rademaker, M.C., de Lange, G.M., Palmen, S.J.M.C., 2018. The Netherlands Brain Bank for psychiatry. Handb. Clin. Neurol. 3–16. https://doi.org/10.1016/B978-0-444-63639-3.00001-3.

Ramirez, E.P.C., Keller, C.E., Vonsattel, J.P., 2018. The New York Brain Bank of Columbia University: practical highlights of 35 years of experience. Handb. Clin. Neurol. 105–118. https://doi.org/10.1016/B978-0-444-63639-3.00008-6.

Ravid, R., Swaab, D.F., 1993. The Netherlands brain bank—a clinico-pathological link in aging and dementia research. J. Neural Transm. Suppl. 39, 143–153.

Rodríguez González, D., Carpenter, T., van Hemert, J.I., Wardlaw, J., 2010. An open source toolkit for medical imaging de-identification. Eur. Radiol. 20, 1896–1904. https://doi.org/10.1007/s00330-010-1745-3.

Samarasekera, N., Salman, R.A.-S., Huitinga, I., Kloueva, N., McLean, C.A., Kretzschmar, H., Smith, C., Ironside, J.W., 2013. Brain banking for neurological disorders. Lancet Neurol. 12, 1096–1105. https://doi.org/10.1016/S1474-4422(13)70202-3.

Scahill, R.I., Frost, C., Jenkins, R., Whitwell, J.L., Rossor, M.N., Fox, N.C., 2003. A longitudinal study of brain volume changes in normal aging using serial registered magnetic resonance imaging. Arch. Neurol. 60 (7), 989–994.

Schroeder, A., Mueller, O., Stocker, S., Salowsky, R., Leiber, M., Gassmann, M., Lightfoot, S., Menzel, W., Granzow, M., Ragg, T., 2006. The RIN: an RNA integrity number for assigning integrity values to RNA measurements. BMC Mol. Biol. 7, 3. https://doi.org/10.1186/1471-2199-7-3.

Shepherd, T.M., Thelwall, P.E., Stanisz, G.J., Blackband, S.J., 2009. Aldehyde fixative solutions alter the water relaxation and diffusion properties of nervous tissue. Magn. Reson. Med. 62, 26–34. https://doi.org/10.1002/mrm.21977.

Smith, C., Millar, T., 2018. Brain donation procedures in the sudden death Brain Bank in Edinburgh. Handb. Clin. Neurol. 150, 17–27. https://doi.org/10.1016/B978-0-444-63639-3.00002-5.

Smith, S.M., Zhang, Y., Jenkinson, M., Chen, J., Matthews, P.M., Federico, A., De Stefano, N., 2002. Accurate, robust, and automated longitudinal and cross-sectional brain change analysis. NeuroImage 17, 479–489.

Sutherland, G.T., Sheedy, D., Stevens, J., McCrossin, T., Smith, C.C., van Roijen, M., Kril, J.J., 2016. The NSW brain tissue resource Centre: Banking for alcohol and major neuropsychiatric disorders research. Alcohol 52, 33–39. https://doi.org/10.1016/j.alcohol.2016.02.005.

Thal, D.R., Rüb, U., Orantes, M., Braak, H., 2002. Phases of a beta-deposition in the human brain and its relevance for the development of AD. Neurology 58, 1791–1800.

van Rooden, S., Maat-Schieman, M.L.C., Nabuurs, R.J.A., van der Weerd, L., van Duijn, S., van Duinen, S.G., Natté, R., van Buchem, M.A., van der Grond, J., 2009. Cerebral amyloidosis: postmortem detection with human 7.0-T MR Imaging System. Radiology 253, 788–796. https://doi.org/10.1148/radiol.2533090490.

van Veluw, S.J., Zwanenburg, J.J., Engelen-Lee, J., Spliet, W.G., Hendrikse, J., Luijten, P.R., Biessels, G.J., 2013. *In Vivo* detection of cerebral cortical microinfarcts with high-resolution 7T MRI. J. Cereb. Blood Flow Metab. 33, 322–329. https://doi.org/10.1038/jcbfm.2012.196.

Vonsattel, J.P.G., del Amaya, M.P., Keller, C.E., 2008. Twenty-first century brain banking. Processing brains for research: the Columbia University methods. Acta Neuropathol. 115, 509–532. https://doi.org/10.1007/s00401-007-0311-9.

Wardlaw, J.M., Smith, E.E., Biessels, G.J., Cordonnier, C., Fazekas, F., Frayne, R., Lindley, R.I., O'Brien, J.T., Barkhof, F., Benavente, O.R., Black, S.E., Brayne, C., Breteler, M., Chabriat, H., DeCarli, C., de Leeuw, F.-E., Doubal, F., Duering, M., Fox, N.C., Greenberg, S., Hachinski, V., Kilimann, I., Mok, V., van Oostenbrugge, R., Pantoni, L., Speck, O., Stephan, B.C.M., Teipel, S., Viswanathan, A., Werring, D., Chen, C., Smith, C., van Buchem, M., Norrving, B., Gorelick, P.B., Dichgans, M., 2013. STandards for reporting vascular changes on nEuroimaging (STRIVE v1), 2013. Neuroimaging standards for research into small vessel disease and its contribution to ageing and neurodegeneration. Lancet Neurol. 12, 822–838. https://doi.org/10.1016/S1474-4422(13)70124-8.

Wisse, L.E.M., Adler, D.H., Ittyerah, R., Pluta, J.B., Robinson, J.L., Schuck, T., Trojanowski, J.Q., Grossman, M., Detre, J.A., Elliott, M.A., Toledo, J.B., Liu, W., Pickup, S., Das, S.R., Wolk, D.A., Yushkevich, P.A., 2016. Comparison of in vivo and ex vivo MRI of the human hippocampal formation in the same subjects. Cereb. Cortex 27, 5185–5196. https://doi.org/10.1093/cercor/bhw299.

Yelnik, J., Bardinet, E., Dormont, D., Malandain, G., Ourselin, S., Tandé, D., Karachi, C., Ayache, N., Cornu, P., Agid, Y., 2007. A three-dimensional, histological and deformable atlas of the human basal ganglia. I. Atlas construction based on immunohistochemical and MRI data. NeuroImage 34, 618–638. https://doi.org/10.1016/J.NEUROIMAGE.2006.09.026.

Yushkevich, P., Avants, B., Pluta, J., Das, S., Minkoff, D., Mechanichamilton, D., Glynn, S., Pickup, S., Liu, W., Gee, J., Grossman, M., Detre, J., 2009. A high-resolution computational atlas of the human hippocampus from postmortem magnetic resonance imaging at 9.4 T. Neuroimage 44, 385–398. https://doi.org/10.1016/j.neuroimage.2008.08.042.